Indian Journal of Biochemistry & Biophysics
Vol. 62, October 2025, pp. 1077-1091
DOI: 10.56042/ijbb.v62i10.16780

Insights into anti-tuberculosis activity of partially purified bioactive fraction from *Vitex negundo* L. petroleum ether extracts against *Mycobacterium smegmatis* - An *in vitro* and *in silico* approach

Sadhana Sundararajan, and Rajiniraja Muniyan*

School of Bio-Sciences and Technology, Vellore Institute of Technology (VIT), Vellore-632 014, Tamil Nadu, India

Received 30 January 2025; *revised 27 June 2025*

The urgent need to search for new anti-TB drugs that are safer and efficient against drug resistant TB have turned towards natural medicine as they contain active ingredients capable of combating the epidemic. Medicinally important plant *Vitex negundo* L. has various health benefits such as anti-inflammatory, hepatoprotective activity and others. However, knowledge on exact compound(s) responsible for anti-TB activity is limited. In this study, partially purified petroleum ether extract of *Vitex negundo* leaves were assessed for its anti-tuberculosis and anti-biofilm activity against *Mycobacterium smegmatis.* Minimal inhibitory concentration of the active fraction was assessed by REMA assay (MIC > 12.5 µg/mL) and time-kill assay (67% inhibition). Anti-biofilm activity was assessed using crystal violet assay (~6.20 µg/mL). Possible compounds from the bioactive fraction were identified using FT-IR and GC-MS analysis displayed presence of classes like terpenoids, flavonoids and alkaloids. These compounds were subsequently docked against cell-wall proteins KasA, MabA, FabD and HadAB of *Mtb* showing HIT 3 was effective in the interaction with all targets. Molecular dynamic simulation of Hit 3 demonstrated a stable interaction with all the target proteins and can be considered as a starting point for developing new drug candidates or as an adjuvant against TB infection.

Keywords: Bacterial disruption, GC-MS analysis, Molecular dynamic simulation, Mycolic acid synthesis proteins, Time-kill assay

More than one quarter of the world population is estimated to be infected with tuberculosis (TB) that is caused by the organism *Mycobacterium tuberculosis (Mtb)* as quoted by World Health Organisation (WHO) Tuberculosis report. It is the most successful single infectious agent to achieve morbid rates above HIV/AIDS[1]. The speciality of the organism is its exquisitely well adapted nature, passing through the innate immune system and enduring in the host with no symptoms until a strong inflammatory response is triggered resulting in significant tissue damage and spread[2].Comprehending the life cycle of *Mtb* is crucial in the development of drugs to combat the epidemic.

Initial TB spreading happens when *Mtb* enters the respiratory tract of the individual. Here, *Mtb* is encountered with alveolar macrophages and dendritic cells for successful phagocytosis. Additionally, traces of neutrophils performing phagocytosis in many cases have been observed. The organisms that escape this initial encounter infects and replicates in the alveolar macrophages. A granuloma is developed by signaling other immune cells to form a cellular aggregate. This is a core pathological marker for TB[3]. Stress conditions such as low oxygen and nutrient availability, created in granuloma, may sometimes force the organism to go dormant or survive and resist immune clearance. The intrinsic adaptation of *Mtb* to replicate inside a macrophage, inhibit phagosome maturation and subvert the production of pro-inflammatory cytokines have also rendered advantageous for disease progression[4].

The complexity of the disease can be attributed to the multifaceted mechanism that promote survival in adverse conditions. This includes the nearly impermeable cell wall composed of hydrophobic mycolic acid units that hinder the diffusion of drugs or any hydrophilic substances across them. Additionally, some actions like enzymatic target modification, improved efflux pump action, gene mutation for drug inactivation, drug target over expression, molecular chaperon activity[5]etc., to evade the immune response and develop resistance to the administered drug. It has been identified in many

*Correspondence:
E-mail: rajiniraja.m@vit.ac.in
Suppl. data available on respective page of NOPR

studies that the organism is an excellent bio-film former which predominantly explains the prolonged treatment time[6].The raise of MDR-TB(Multi-drug resistant TB) and XDR-TB(Extreme-drug resistant TB) has complicated the situation and extended the treatment period upto 20 months and requires use of highly toxic, expensive and relatively less effective second line drugs[7]. However, the success in treating MDR and XDR-TB have rendered low so far.

To overcome the above discussed hurdles, there is an urgent need of an alternate therapy that can be less toxic but has improved efficiency. Despite the success of natural compounds such as nicotinamide (basic compound for isoniazid) and rifamycin (basis for rifampicin) and some second-class antibiotics that also include natural compound derivatives, many natural compounds are still unexplored as anti-TB agents except a few herbal formulations prescribed in Ayurvedic and Chinese medicine. Interestingly, no new biological compound has been commercialized since the discovery of rifampicin[8]. However, the FDA has approved a list of natural products derived drugs for treatment of TB and associated diseases that are yet to make it to the market[9]. This gives scope forexploring plants further based on their ethnobotanical usage to identify new compounds to treat TB.

Vitex negundo L. (Lamiaceae) referred as Vn in this study, is a traditional plant known as five-leaved chaste tree for its diverse medicinal uses found across Asia, North America, Europe, and the West Indies. This plant's parts are rich in various bioactive compounds like lignans, iridoids, terpenes, flavonoids, and steroids. It is credited with intense hepatoprotective, anti-inflammatory, antioxidant, antidiabetic and antimicrobial benefits. It also plays a role in regulating apoptosis and cell cycle regulation[10]. The involvement of phytochemicals from Vn in treating internal injuries, bronchitis, asthma, oral ulcers, rheumatism by formulation of decoctions and pastes[11] have further drawn attention towards exploring the effect of Vn in treating tuberculosis.

Mycobacterium smegmatis (*M. smegmatis*), a non-pathogenic fast-growing mycobacterium with genetic makeup that can be closely related to *Mtb* in terms of drug susceptibility pattern, is studied. Screening phytochemicals against *Mtb* can be an aseptically rigorous process with concern to its extremely infective, slow growing (generation time 14-24 h) and deadly nature[12]. This slow growing – highly pathogenic nature of *Mtb* has also slowed down the progress of anti-TB drug discovery. Hence, preliminary drug screening is generally done in *M. smegmatis.*

Recently, approaches where targeting more than one protein to certainly overpower the organism are being undertaken widely[13]. The fatty acid synthase (FAS) system I and II, equally contribute in synthesis and elongation of fatty acid units in *Mtb*. Among them, four discrete proteins that are central point for mycolic acid synthesis are chosen for this study, namely KasA, MabA, HadAB and FabD. The inactivation of any of the four enzymes in the complex has been proven to greatly hinder the process of mycolic acid synthesis[14]. Hence these proteins might be marked as ideal drug targets. HadAB complex performs action similar to KasA by synthesis and elongation of early mero-mycolic acid. HadBC complex performs action like KasB which is the elongation of medium size mero-mycolic acid units. FabD serves as a branching point between KasA/B and HadAB[15].

This study aims in screening organic extracts of *Vitex negundo* L. against *M. smegmatis* to identify compounds with potential anti-mycobacterial properties. The partially purified fraction of Vn is assessed by various parameters such as resazurin microtiter assay (REMA), minimal inhibitory concentration (MIC) determination, time-kill assay and anti-biofilm assay, to determine its anti-TB activity. The fraction showed commendable anti-TB activity suggesting its potential as a starting point for developing a therapeutic agent. To further validate its efficacy, *in silico* analysis of the compounds against important protein targets of *Mtb* that are involved in cell wall synthesis were performed.

Materials and Methods

Sample collection and serial extraction

Vitex negundo leaves were collected from Vellore region during August-September and identified by Dr. C. Rajasekaran, professor (Botanist) at Vellore Institute of Technology. A specimen bearing the voucher number VITMN066-1 was preserved in the VIT herbarium. The plant used in this study is neither endangered nor protected species.

The leaves were washed with deionised water and dried under shade. Dried leaves were ground to fine powder and stored under dry condition. 20 g of powdered plant sample was extracted using Soxhlet method with various solvents of increasing polarity *viz*, petroleum ether, chloroform, ethyl acetate and

methanol to their heating point for about ~20 h each[16]. The obtained crude mixtures were filtered and concentrated by distillation and stored for further analysis. The crude was tested against *M. smegmatis* at ~1mg/mL concentration, using agar well diffusion assay. Positive control was rifampicin 5 µg and the respective solvents maintained as negative control. The inhibitory activity of the crude extracts was determined qualitatively by observing the zone of inhibition in terms of mm in diameter.

Bacterial culture

The *M. smegmatis* culture (MTCC 6) was commercially acquired from Microbial Type Cell Culture (MTCC), Chandigarh, India. The bacteria were maintained in 37°C after culturing in Middlebrook 7H9 medium, supplemented with 0.5% glycerol and grown in a shaker incubator at 37°C at 120 rpm until optical density (OD_{600}) reaches 0.8[17].

Phytochemical analysis

Phytochemical analysis for bioactive petroleum ether extract of Vn was done based on results from agar well diffusion assay as described by[18] with slight modifications and the results are included in (Suppl. Table 1).

Extraction and fractionization of bioactive compounds

The bioactive petroleum ether extract was subjected to column chromatography. Briefly, 20 grams of petroleum ether extract was evenly packed on to a vertical glass column with silica gel (60-120 mesh). Fractions were collected at the rate of 1 mL/min and fractions with sameretention factor (Rf) values and UV-spectrophotometric profiles were pooled. The crude sample and fractions were separately subjected to TLC (Merck, F254) with solventsxylene: dichloromethane in the ratio 0.5mL: 4.5 mL for petroleum ether crude extract. For column fractions collected, best separation was seen with petroleum ether: chloroform in the ratio 1mL: 4mL in developing chamber. The bands were visualised under UV (254 nm and 360 nm) and Rf values were calculated[19].

Contact bioautography

Plates pre-seeded with *M. smegmatis* grown in 7H9 medium supplemented with glycerol were prepared and fractions in TLC plates were allowed to develop in corresponding solvent systems. The TLC plates were allowed to dry and then placed face-down on the surface of agar. The TLC sheets were removed after 40 m and the plates were sealed and incubated at 37°C for 48 h[20]. The bioactive fraction showing anti-TB activity was inferred by formation of clear zone around the band. The Rf value of the corresponding band was determined.

Ultra performance liquid chromatography

Ultra Performance Liquid Chromatography (UPLC) analysis of active fraction was performed as described by[21] with modifications. UPLC was done using Acquity-H class equipped with PDA detector instrument equipped with C18 column (particle size 2.5 µm, column length 150 mm). Mobile phase used was methanol (B) and 1% acetic acid (A). 50 µL of sample was passed through C18 column and fractions were collected at rate of 1 mL/min. The temperature of the setup was ~30°C. Detection was done using UV detector with range set to 200 nm – 800 nm. All the samples and solvents were filtered prior analysis. The gradient system was as follows: 0-10 m – 25% B; 10-20 m – 50% B; 20-30 m – 75% B; 30-40 m – 100% B with a total run time was 40 m.

Fourier transform infrared spectroscopy

The bioactive fraction collected from UPLC designated as VnPeF1, was subjected to Fourier transform infrared spectroscopy (FT-IR) analysis on Jasco FT-IR/FT-NIR-6800 spectrometer. Sample was analysed in attenuated total reflection (ATR) mode. A resolution of 4 cm^{-1} and a scanning range of 500 to 4000 cm^{-1} was set. Resulting peaks were compared to literature for identification of potential functional groups[22].

Resazurin microtiter assay

The REMA assay, as outlined by[23] was used to ascertain the minimum inhibitory concentration (MIC) of VnPeF1 against *M. smegmatis*. The wells were filled by dispensing 80 µL of Middlebrook 7H9 broth into of a 96-well plate. FractionVnPeF1was dissolved in DMSO and serially diluted from 100 µg/mL to 0.2 µg/mL concentration. 50 µL of this serially diluted compound fraction was added into the wells. An untreated control was maintained to assess the growth devoid of any treatment. Positive control used was 5 µg rifampicin and negative control used was DMSO. The experiment was performed in triplicates, sealed and incubated for 48 h at 37°C. After incubation, 20 µL of 0.04% (0.04 g in 100 mL) resazurin dye was freshly prepared and added in all the wells and further incubated for 24 h. A change in colour from blue to pink indicated bacterial growth. MIC can be regarded as the minimum concentration of drug required to inhibit bacterial growth indicated by preventing the colour change in resazurin solution.

***In vitro* time-kill assay**

Time-kill assay was conducted with modifications from[24] *M. smegmatis* was cultured overnight in 7H9 media at 37°C and let to grow until it reached log phase. VnPeF1 was prepared by double dilution method similar to REMA assay (100 µg/mL to 0.2 µg/mL) and added to 96-well microtiter plates in triplicates, along with 5 µg/mL rifampicin (positive control). A 30 µL of bacterial inoculum was added to all wells and incubated overnight at 37°C. At specified time points (0, 2, 4, 6, 8, and 24 h), the bacterial population was quantified by measuring OD at 600 nm. A simultaneous negative control and an untreated control were also maintained. The percentage reduction from the initial microbial population was calculated for each time point to assess the effect of the extract, using the formula as given below;

$$\text{Percentage growth inhibition}=\frac{\text{Mean OD of control-Mean OD of test}}{\text{Mean OD of control}}\times 100$$

Biofilm inhibition assay

The ability of VnPeF1 to inhibit biofilms was tested against *M. smegmatis,* a known biofilm-former. The experiment was done as described by[25] with slight modifications. A 60 µL *M. smegmatis* inoculum was added to a 96-well microplate, followed by the addition of various concentrations of VnPeF1 starting from 100 µg/mL to 0.78µg/mL by double dilution method. A positive control (rifampicin 5 µg) and a negative control (culture, samples, broth, and solvent) were maintained simultaneously. The plates were incubated at 37°C for 48 h in stationary condition to induce biofilm formation. The culture was drawn out from the wells after 48 h and plate was washed with distilled water twice to remove planktonic cells and allowed to dry. The biofilm was then stained with 0.1% crystal violet solution (250 µL) and allowed to stand for 20 m. The plate was washed with distilled water and dried. 95% ethanol was added to dissolve the biofilm and allowed to stand for 20 m. The amount of bound crystal violet was measured using a plate reader (Agilent technologies) at OD_{595} nm to determine the biofilm biomass. The percentage of biofilm inhibition was calculated using the same formula as given below;

$$\text{Percentage biofilm inhibition}=\frac{\text{Mean OD of control-Mean OD of test}}{\text{Mean OD of control}}\times 100$$

Gas chromatography-mass spectrometry analysis

Gas chromatography Mass spectrometry (GC-MS) analysis is done to identify small molecules and volatile compounds at high accuracy from plant samples. GC-MS analysis was done at the Central Instrumentation Facility of the Indian Institute of Science (IISc), Bangalore, India. The instrument setup included a Shimadzu gas chromatograph (GC) equipped with an Agilent 7890 A system and a mass spectrometer (MS) with a 5975C detector. The MS operated using electron impact ionization, and the mass analyser employed a quadrupole configuration. The chromatographic column was an HP 5 MS column (30 m length × 0.25 mm inner diameter × 0.25 µM film thickness). The temperature program involved an initial ramp from 0°C to 400°C over 2 m, followed by a hold at 310°C for 10 m. Helium served as the carrier gas (flow rate: 1.0 mL/min). Sample injection volume was 10 µL, and the scan mass range covered 200 *m/z* to 400 *m/z* in positive polarity. The unknown compound's mass spectrum was compared with known compounds in the NIST library (National Institute of Standards and Technology, USA) at IISc, Bangalore, India[26].

***In silico* analysis**

Ligand and protein preparation

The three-dimensional proteins structures were retrieved from PDB (https://www.rcsb.org/) after checking for resolution, missing residues and mutations. All the structures obtained had a resolution of about 2 Å with no mutations. The active sites of the proteins were identified from literature[13]. The PDB ID of the proteins considered for this study are included in (Table 1).

Table 1 — PDB ID and function of proteins considered in this study

S.no.		Name	Function	PDB ID
1	KasA/B	Beta keto acyl ACP synthase	Synthesis and elongation of mero- mycolic acid fragments	2WGE
2	MabA	Beta keto acyl reductase	Reduction of B-keto acyl ACP	1UZL
3	FabD	Malonyl CoA Acyl carrier protein transacylase	Branching point between FAS-I and FAS-II system	2QC3
4	HadAB	Beta ketoacyl ACP dehydratase	Catalysis of initial mero-mycolic acid chain elongation	4RLW

Virtual screening

The compounds predicted from GC-MS analysis of VnPeF1 were obtained from PubChem database in sdf format and converted into pdbqt format using openbabel 3.1.1[27]. The compounds were subjected to fast rank screening using AutoDock Vina 1.1.2[28]. Grid box was formed focusing on the active sites of proteins obtained from literature. The protein complexes that had highest binding affinity were filtered and taken for exhaustive docking. All the compounds used in this study were passed through Lipinski's filters and ADMET filters using DruLito server and DataWarrior application[29].

Exhaustive docking

Molecular Docking was done with AutoDock 4.2 for the compounds based on its binding energy and interaction sites. Exhaustive docking for 100 iterations with the grid parameters maintained the same as virtual screening was done. Results were analysed in Discovery studio visualise for binding affinity, poses and interaction with the key residues. The most prominent hit in terms of interaction and binding energy were further subjected to molecular dynamic simulation[28].

Molecular dynamic simulation

In order to gain insights on the changes upon ligand binding to the protein, an atomic level analysis of the protein is done using molecular dynamic simulation (MDS). Hit compounds were simulated with the *Mtb* proteins (FabD, HadAB, MabA and KasA) along with apo-proteins, in Gromacs version 2023.1[30]. Protein topology was created using Charm27 and ligand topology was obtained from SwissParam server[31]. The protein was situated in a cubic box with a 1 cm dimension and solvated using SPC (simple point charge). The simulation conditions included a 0.15M NaCl concentration, 1.0 bar pressure, and a constant temperature of 300 K. Energy minimization of 50,000 steps were done. The simulation was set for 100 ns and the analysis was done using Xmgrace.

Results

Serial extraction

The petroleum ether extract and methanol extracts from serial extraction, had considerable activity against *M. smegmatis* in agar well diffusion assay. However, in this study, crude of petroleum ether extract was taken for further analysis, based on its excellent anti-mycobacterial activity as shown in (Table 2). The results obtained were compared to earlier studies where crude extracts of the plant as well as individual compounds identified from the plant have multiple advantages in breathing related ailments[32].

Phytochemical screening

Petroleum ether extract of Vn was further assessed using a qualitative phytochemical analysis to detect the classes of possible compounds. The results displayed the presence of diverse range of phytochemical classes (Suppl. Table 1). Alkaloids, terpenoids, fats and fixed oils were prominently identified in the extract. Petroleum ether being a low polarity solvent, has the tendency to attract compounds with hydrocarbon rings and odd number carbon containing compounds.

Purification using thin layer chromatography and column chromatography

Thin layer chromatography was done in petroleum ether sample crude(VnPe) with solvents xylene: dichloromethane in ratio 0.5 mL:4.5 mL. Four bands with Rf values 0.084, 0.16, 0.3 and 0.4 were observed after development and drying (Suppl. Fig. S1).The limited movement of compounds from the initial point, suggests that the compounds can be highly polar in nature. The compounds of the Vn Pe extract were separated in isocratic method using column chromatography technique with xylene: dichloromethane as mobile phase. Fractions collected were categorised and pooled into 3 batches F1, F2 and F3 based on the UV spectrophotometric profiles and similarity in Rf values in TLC analysis. When subjected to anti-mycobacterial agar well diffusion assay, VnPeF1 was found to be the most active

Table 2 — Antimycobacterial activity of various solvent extracts of *Vitex negundo* against *M. smegmatis* using agar well diffusion assay

Plant name	Extract	Concentration	Zone of inhibition (mm in dia)	Positive control (rif 5 µg)	Negative control
Vitex negundo	Petroleum ether	1 mg/mL	8.7±0.81	5.6	Nil
	Chloroform		Nil	5.4	Nil
	Ethyl acetate		8.3±0.36	5.5	Nil
	Methanol		7.2±0.35	6.2	Nil

fraction while the other batches lacked any activity against *M. smegmatis.*

Contact bioautography and UV spectrometric analysis of active fraction

The bioactive fraction VnPeF1 was analysed further using TLC for detailed examination of compounds in the fraction in attempt to identify exact compound class that may be responsible for the anti-mycobacterial activity of the particular fraction. The TLC of VnPeF1 fraction was done with solvents petroleum ether: chloroform in the ratio 1: 4.

The sample VnPeF1 was analyzed using contact bioautography to narrow down the band that has bio activity. The F1 fraction was run in a TLC plate, dried and then inverted over a plate of agar pre-seeded with *M. smegmatis.* The results of contact bioautography showed that the first band of VnPeF1 had anti-TB activity. A clear zone was seen around the first band with Rf value 0.4. This fraction was designated as FB3 as highlighted in (Fig. 1). The part FB3, which is the active band of VnPeF1, was dissolved in methanol and analyzed using UV spectrophotometer with range set from 200- 800 nm. Upon drying, FB3 was a colorless and odorless amorphous solid. The compounds of FB3 showed an absorption maxima (λ_{max}) at 219 and 246 nm (in methanol). The peak at around 246 nm suggests the presence of aromatic rings in the structure.

Ultra performance liquid chromatography

The fraction VnPeF1 was analysed using UPLC showed single most prominent peak at 33.7 retention time (Rt). Simultaneously, the active band FB3 obtained from contact bioautography was also analysed in UPLC under the same conditions to compare the peaks appearing. Both the samples showed a single most prominent peak at 33 to 36 Rt

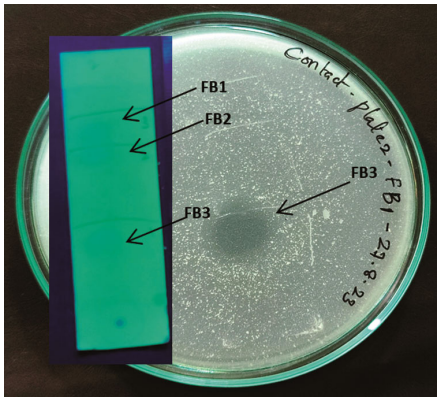

Fig. 1 — Contact bioautography of column fraction VnPeF1 showing active band FB3 with anti-TB activity

with similar absorbance maxima at ~235 nm to 245 nm. Hence the peak appearing at 33.7 Rt of VnPeF1 and peak appearing at 36.5 Rt of FB3 samples can be considered to contain the same compounds. This fraction particularly showed inhibitory activity as observed in contact bioautography. Therefore, based on the observation the peak appearing at 33.7 Rt from VnPeF1was collected from UPLC and analysed further using FT-IR and GC-MS to identify the plausible active compounds and their functional groups. The UPLC chromatogram of VnPeF1 and FB3 are given in (Fig. 2).

Fourier transform infrared spectroscopy

FT-IR is a highly sensitive tool used for the identification of functional groups in any unknown plant extract. It helps in identification and structure determination of a molecule. FT-IR analysis of VnPeF1 revealed the presence of -OH stretch group indicated by a prominent broad strong peak at 3321 cm^{-1}, a weak peak at 2623 cm^{-1}, aromatic overtones at the range 2355- 2198 cm^{-1}, a medium intensity sharp peak at 1649 cm^{-1} suggests that aromatic ring is present in the structure. A weak peak in the area 1388 cm^{-1} suggests the presence of nitrate ion conjugated with aromatic ring. The weak peak at 1016 cm^{-1} indicates the presence of -C-O stretch and wide peak at 580 cm^{-1} suggests the presence of aromatic ring. The FT-IR chromatogram representation of VnPeF1 is given in (Fig. 3).

Resazurin microtiter plate assay

The MIC of fraction VnPeF1 was screened for anti-tuberculosis activity using resazurin to indicate the viability of *M. smegmatis* in a 96-well plate. The MIC of the bioactive compound had a range from 12.5 µg/mL to 100 µg/mL as shown in (Fig. 4). However, partial mycobacterial inhibition was also observed in some concentrations like 6.25 µg/mL and 0.78 µg/mL identified by colour change after 24 h of incubation with resazurin. An intense blue to purple colour was observed from the wells with concentration 12.5 µg/mL upto 100 µg/mL confirmed the complete inhibition of bacterial growth effected by the compound. From the analysis, the MIC of the compound against *M. smegmatis* could be concluded as 12.5 µg/mL on comparison with untreated wells.

***In vitro* time-kill assay**

Time dependent kill assay was carried out to identify the killing capacity of the extract VnPeF1. The bactericidal activity was observed to be highly time and concentration dependent. Maximum

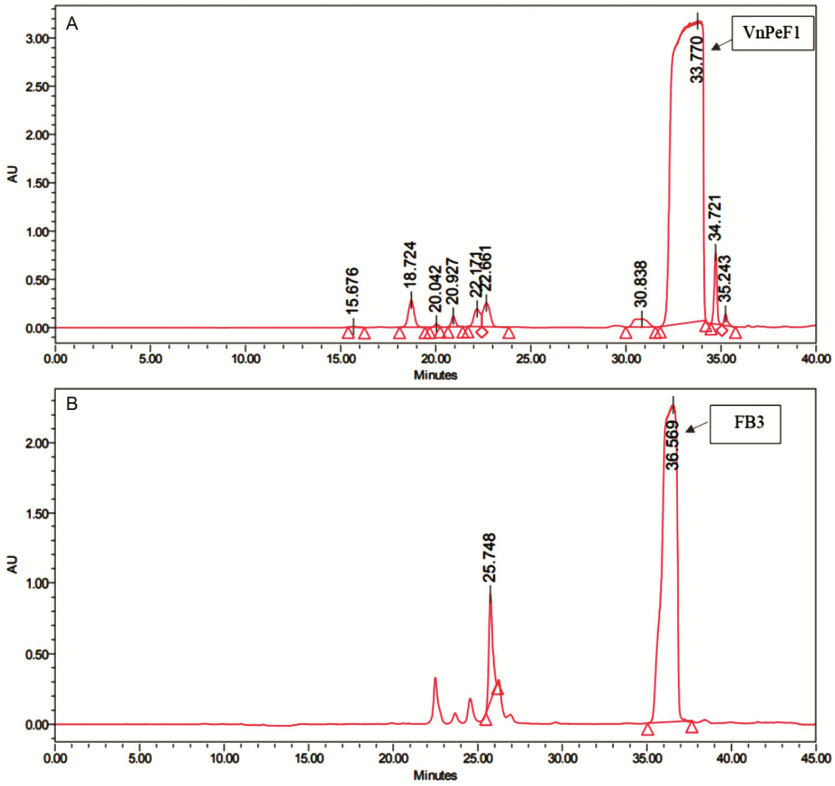

Fig. 2 — UPLC chromatogram showing of (A) VnPeF1; and (B) FB3 showing single most prominent peak of possibly similar compounds

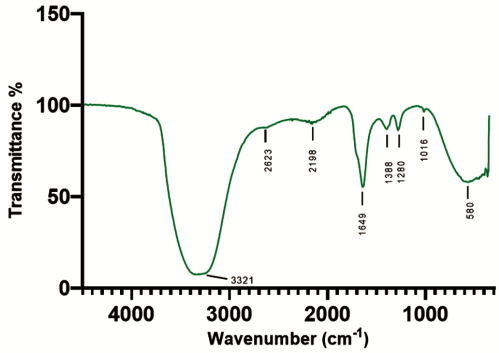

Fig. 3 — FT-IR data of active fraction VnPeF1 in ATR mode.

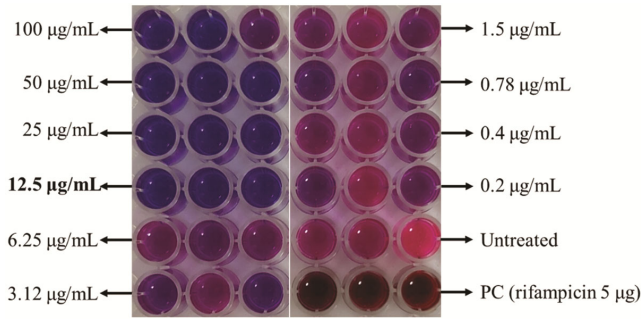

Fig. 4 — anti-mycobacterial effect of active fraction VnPeF1 showing minimal inhibitory concentration at 12.5 µg/mL. Pink wells represent absence of inhibition and blue wells represent active bacterial inhibition. Experiments performed in triplicates

inhibition of 67% was achieved at the concentration of 50 µg/mL after 8 h of incubation with the compound. Overall, the various concentrations of compound were seen to be most active in mycobacterial inhibitory activity at the 8 h. Regardless of the concentration, the compound behaved in a similar fashion until 6 h. But there was a sudden shift in activity at the 8 h in 50 µg/mL whereas the other lower concentrations such as 12.5 µg/mL (50% inhibition), 6.25 µg/mL (46% inhibition) and 0.78 µg/mL (48% inhibition) also behaved in a similar pattern but with lower killing intensity. From the study, it could be clearly seen that 50 µg/mLhad the maximum inhibitory activity against *M. smegmatis*. This is also in alignment with the results obtained from REMA assay where minimum inhibitory concentration was identified in concentrations as low as12.5 µg/mL. The time dependent killcurve of VnPeF1 against *M. smegmatis* is given in the (Fig. 5).

Biofilm inhibition assay

Biofilm inhibition was studied in a dose dependent manner where the maximum inhibition with statistical significance was observed at a concentration of 6.25µg/mL showing 54% inhibition. However, higher concentrations of the compound did not affect the

biofilm formation considerably as the growth of the organism itself at higher concentrations would be hindered. When the obtained values were compared with positive control (rifampicin 5 µg/mL), the partially purified extract, VnPeF1 showed better anti-biofilm activity indicating the efficiency of lower concentrations of VnPeF1. However, there was no complete inhibition of biofilm formation at any given concentration. The anti-biofilm effect of VnPeF1 is shown in (Fig. 6).

GC-MS analysis

GC-MS analysis of VnPeF1 enabled the identification of various phytochemicals. The compounds predicted fell into main classes of alkaloids, anthraquinones, organosulfur, terpenoids, and flavone phytochemicals that show high biological significance. The chromatogram obtained from GC-MS analysis is represented in (Fig. 7). The major compounds identified using GC-MS are listed in (Table 3).

***In silico* analysis**

Virtual screening

Compounds predicted from GC-MS analysis were converted to pdbqt format and passed through Lipinski's rule and toxicity filters. A total of nine compounds were virtually screened against the four selected proteins of *Mtb*. The results were arranged in order of their binding energy. The top three hit compounds with prominent binding energy and key residue interaction were chosen and further analysed by exhaustive docking. All the compounds considered for the study passed the multi-filtration steps of Lipinski's rule and toxicity.

Exhaustive docking and post-docking analysis

The compounds that passed with not less than 2 filters of the multi-filtration steps of virtual screening were taken for exhaustive docking with 100 iterations. Hit 1, Hit 2, Hit3, Hit4 and Hit 9 seemed to

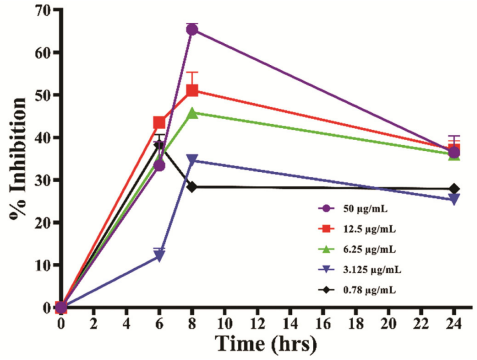

Fig. 5 — Time dependent and concentration dependent anti-tuberculosis activity of VnPeF1 extract on *M. smegmatis*. The graph highlights concentrations 50 µg/mL, 12.5 µg/mL, 6.25 µg/mL, 3.125 µg/mL and 0.78 µg/mL of sample at various time intervals. (p- value < 0.002, significance - ***). Values are the mean of ± SD for N = 3

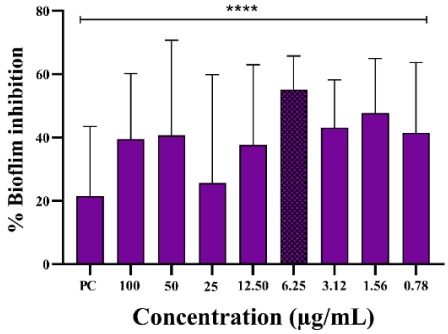

Fig. 6 — Anti-biofilm potential of VnPeF1, showing maximum inhibition of ~54% at concentration 6.20 µg/mL. (p- value: < 0.0001, significance: ****). Values are the mean of ± SD for N = 3

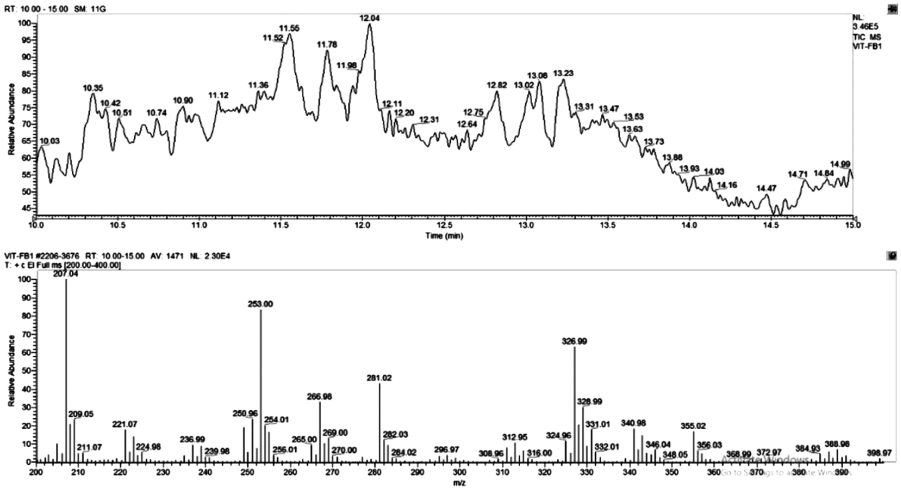

Fig. 7 — Gas Chromatography-Mass Spectrometry analysis of partially purified petroleum ether extract fraction of *Vitex negundo*

Table 3 — Possible list of compounds identified using GC-MS identified from VnPeF1

S. No	Compound name	Retention time	Molecular weight (Da)	Molecular formula
1	9,10-Anthracenedione, 1,8-dimethoxy	10.03	268.04	C16H12O4
2	1,5-Diphenyl-2H-1,2,4-triazoline-3-thione	10.35, 12.51	253	C14H11N3S
3	1,2-Dicarboxy-3-(4-chlorophenyl)-2,3(1H)-dihydropyrido(1,2-a)benzimidazole	10.51	370	C19H15ClN2O4
4	Benzenesulfonamide, N-(3-chloro-1,1-dioxo-1,2-dihydro-1.lambda.(6)-naphtho[1,8-cd]isothiazol-5-yl)-4-methyl	10.51	408	C17H13ClN2O4S2
5	Schizandrin B	10.74	400	C23H28O6
6	7,8,4'-Trihydroxyisoflavone	11.55	270	C15H10O5
7	Carbamazepine 10,11-epoxide	12.04	253	C15H12N2O2
8	Iridin	13.08	522	C24H26O13
9	Spironolactone	15.28	416	C24H32O4S

Table 4 — Binding energy and interacting residues of Hit 3 against *Mtb* proteins

S. No	Protein name	Binding energy (kcal/mol)	Active site residues
1.	KasA/B	-12.49	Pro280, Gly318, Phe402, Phe237, Ala279, Gly403, Phe404, Asp273, His311, His345
2.	MabA	-15.21	Ser140, Val141, Other interactions: Val62, Gly28, Ala89, Leu21, Arg47, Ala111, Gly90, Ser140
3.	FabD	-11.07	Gln 9, His 194, Ser 91, Arg 116
4.	HadAB	-12.54	Asp36, Gly59, His41, Met60, Asn38, Gln68, Leu142, His58, Tyr65, Gln86

perform well in comparison with the other compounds from the list. Hit3 (3-chloro-N-[2,3-dihydro-1,4-benzodioxan-6-yl)-1,3-thiazol-2-yl]benzenesulfonamide) had common interaction with all the selected proteins with higher binding affinity and interaction with almost every key residue in all the proteins. Hence, Hit 3 was taken for MDS analysis. The results of exhaustive docking analysis of Hit3 with *Mtb* proteins are given in the (Table 4 and Suppl. Fig 2).

Molecular dynamic simulation

Frequent point mutational and conformational changes in the proteins of *Mtb* contribute to the resistance to first line and second line drugs. Hence, the dynamic of the protein upon binding of the compound must be stable to be considered as a successful lead. Furthermore, since docking studies deal with protein being kept rigid, it is important to study and analyse the protein bound complex in dynamic environment to mimic the biological system. MDS for the compound (Hit3) with proteins HadAB, FabD, MabA, and KasA along with apo-proteins were performed for 100 ns. Various parameters such as intermolecular hydrogen bonding, RMSD (Root mean square deviation), RMSF (Root mean square fluctuation), SASA (solvent accessible surface area) and Rg (radius of gyration) were analysed. Overall, these parameters were compared to the apo-protein for the stability upon compound binding.

Hit 3 compound stabilised the protein FabD after its binding. Throughout the simulation process, a stable behaviour was observed with average RMSD not above 0.2 nm. RMSF pattern of the protein after binding was stabilised with fluctuations in the loop regions on comparison with the apo-protein. The active sites of the protein were located far from the regions carrying the fluctuations. Rg and SASA are measured in terms of lower average values indicating the rigidity and folding of the protein. The protein FabD had an average Rg value of 1.88 nm and SASA value of 131 nm indicating that the ligand binding has stabilised the protein on comparison with its free form. However, the pattern does not drastically vary for apo-protein and bound form. The representation of protein complex is given in (Fig. 8A).

For the protein MabA, average RMSD value was 0.15 nm showing not much of a stable interaction throughout the simulation especially from 22 to 35 ns. However, it gains stability in the second 50 ns than free MabA. RMSF is seen to be in similar fashion for both free and bound protein with significant decrease in the fluctuation intensity when complex is bound. The average Rg value and SASA values decreased in complex form, indicating the improvement in integrity

of protein after binding with Hit3.The illustration of protein behaviour is given in the (Fig. 8B).

KasA is a 416 amino acid containing protein. Upon interaction with compound, the RMSD of the complex decreased drastically after 30 ns and attained stability throughout the simulation with an averageof 0.19 nm. The average RMSF value was 0.08 nm, following almost the same pattern of the apo-protein but with less intensity than the former. The fluctuations are seen mainly in loop regions away from the active site. The representation of protein stability is given in (Fig. 8C).

HadAB interacted well with Hit 3 in MDS. It stabilised the protein upon binding which can be seen in stable RMSD value 0.15 nm. The RMSD graph of the complex stabilised gradually, with minor fluctuations from 30- 40 ns when compared with the apo-protein. The RMSF value of the complex is comparatively lower than free form of protein with an average of 0.08 nm. The Rg and SASA parameters of the protein behaved almost the same attaining drastically stable conformation after the compound binding. The illustration of HadAB interaction with Hit3 is given in the (Fig. 8D).

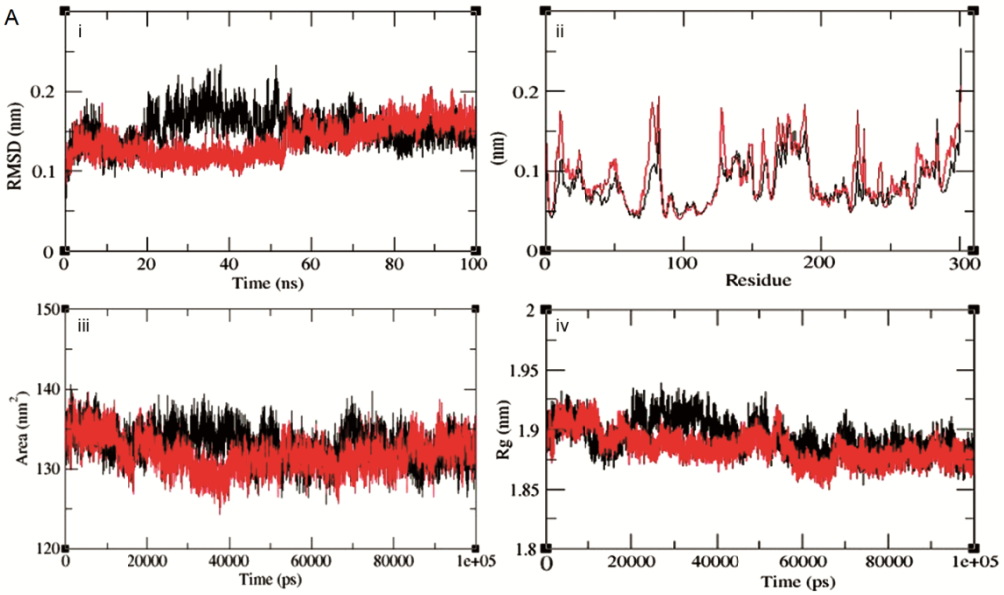

Fig. 8A — Interaction of FabD with Hit 3. (A) RMSD, (B) RMSF, (C) SASA and (D) Rg

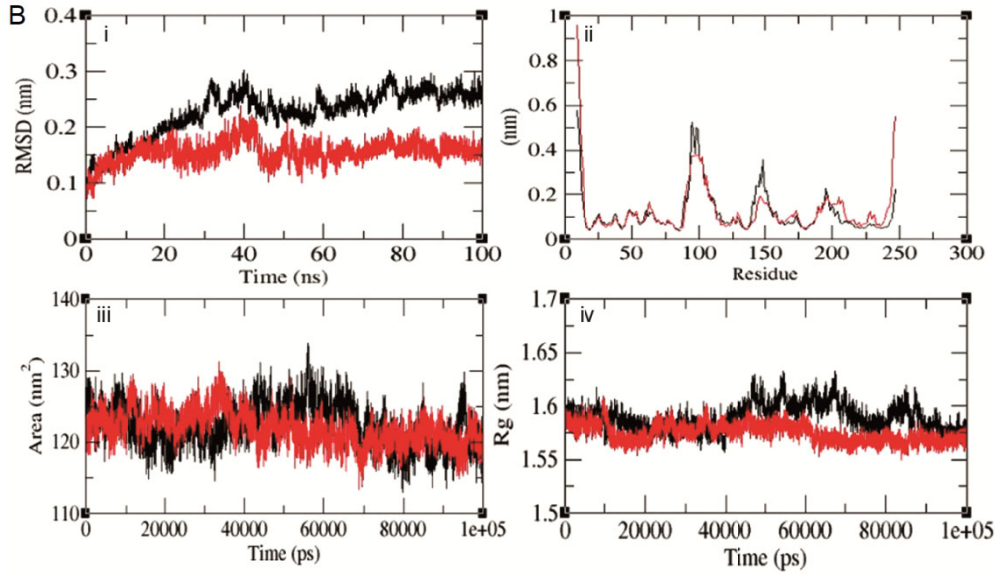

Fig. 8B — Interaction of MabA with Hit 3. (A) RMSD, (B) RMSF, (C) SASA and (D) Rg

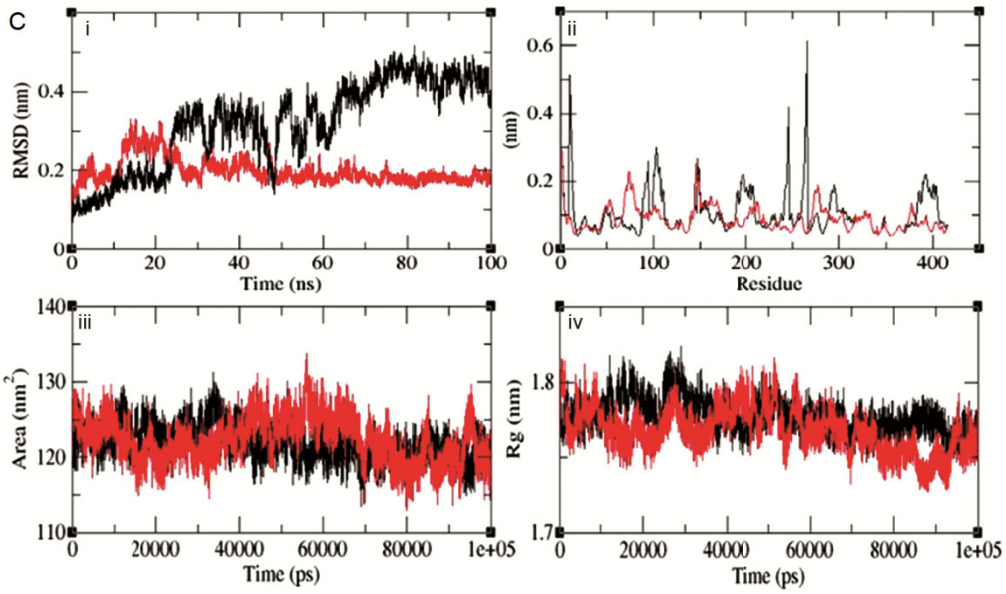

Fig. 8C — Interaction of KasA with Hit 3. (A) RMSD, (B) RMSF, (C) SASA and (D) Rg

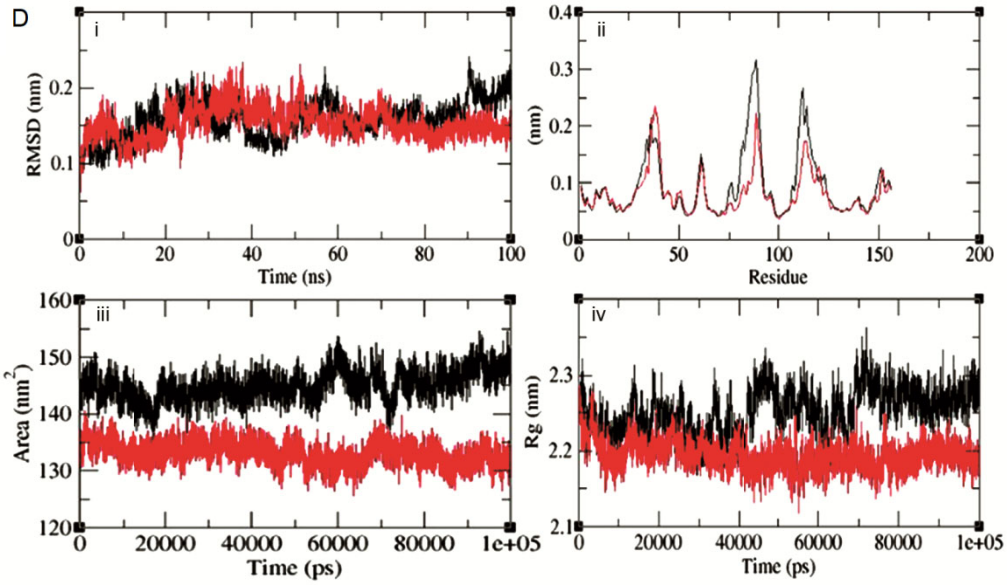

Fig. 8D — Interaction of HadAB with Hit 3. (A) RMSD, (B) RMSF, (C) SASA and (D) Rg

The formation of hydrogen bonds is the parameter used to analyse the compactness and stability of protein complex. In this study, it is observed that the number of hydrogen bonds can be directly co-related with the RMSD, RMSF, Rg and SASA to arrive at a conclusion that the Hit 3 compound behaves rigid with all the proteins chosen for the study. The number of H-bonds range from 2-5 in number, with protein MabA showing 4 H-bonds, protein FabD formed with 5 H-bonds, protein KasA forming upto 2 H-bonds and HadAB formed 4 H-bonds. The H-bond representation of the proteins with the Hit 3 is given in (Suppl. Fig. S3).

Discussion

The urgent need for effective anti-microbials to combat drug resistance and rapidly treat microbial infections requires the discovery of new pharmaceuticals. This demands a collaborative effort between various aspects of science to identify and

validate bioactive molecules from traditional plants. Unfortunately, pharmaceutical industries have been slow to develop new antimicrobial agents, leading to overreliance on existing antibiotics and the rise of drug resistance. Also, the possibility of resistance to natural compounds are less because of their complexity and variety in structure[33].

The objective of the study was to investigate anti-mycobacterial effect of petroleum ether extract of *Vitex negundo* L., a traditional medicine used in treating severe cough, bronchitis and respiratory infections. It is proven to have remarkable hepatoprotective activity by various *in vitro* experimental studies[34]. A study conducted by[35] identified that crude extracts of Vn showed activity against clinical strains of *M. smegmatis* and *Mtb in vitro* and *in vivo.* In another study dealing with various crude extracts of Vn carried out by[16] it was concluded that phytochemicals like β-sitosterol, betulinic acid and ursolic acid along with other few phytochemicals had considerable anti-TB activity. The rich bio-activity of this plant extracts may be corresponded to the plethora of phytochemical classes found in it. Predominantly, alkaloids, flavonoids, terpenoids, glycosides, phenolic acids etc., are the classes of phytochemicals seen in the plant[36].

In our study, petroleum ether extract of the plant leaves displayed major phytochemical classes coinciding with earlier reports. The bioactive fraction identified was a colourless odourless solid that showed UV absorption maxima at ~219 nm and ~247 nm (in methanol) suggesting the presence of aromatic structure in the compound. Further FTIR analysis showed OH group presence (3321 cm^{-1}), aromatic overtones (2355 to2198 cm^{-1}), an aromatic peak represented at 1649 cm^{1}, a possible nitrate ion presence (1388 cm^{-1}) that is conjugated with the aromatic ring, C-O stretch peak at 1016 cm^{-1} and wide peak at 580 cm^{-1} suggests the presence of aromatic compounds[37,38].

It is said that any compound/extract that inhibits mycobacterial growth above 50% at concentration less than 100 µg/mL is considered effective. *Mtb* generally shows resistance to compounds and antibiotics at concentration above 100 µg/mL[39]. A striking factor about *Mtb* is the ability to form biofilms as clumps called chords, that correlate with its virulence. In this study, a strong anti-biofilm effect of VnPeF1 on *M. smegmatis* is a compelling evidence that the compound mixture has an impact on the persistence of the bacteria[40]. The extract showed efficient inhibition at concentration as low as 12.5 µg/mL in REMA assay. This can be seen parallel with time dependent kill curve where, a prominent loss of bacterial activity was observed at 8 h post incubation in the concentration of 50 µg/mL while a partial loss of activity was observed in the concentration 12.5 µg/mL. Irrespective of the concentration, the compound behaved similar until 6 h and at24 h post incubation. There are very few studies that show effect of crude extracts of Vn on MDR strains of *Mtb*[41]. However, there are no extensive reportsof time kill assay, MIC and anti-biofilm activity of partially purified compounds identified from the leaf extract against *M. smegmatis.* Despite having excellent anti-mycobacterial activity accessed by REMA, the inhibition activity of the compound at higher concentrations (100 µg/mL) was lesser as observed in time-kill assay. This might be reasoned as biphasic effect where few compounds by their nature might trigger stress response in the bacteria at elevated concentration. Thereby leading to adverse effects such as growth enhancement, biofilm formation *etc*., [7].A62% biofilm inhibition at a relatively lower concentration of 6.2 µg/mL was also observed. *Mtb* can evade the host's immune system and establish persistent infections by forming biofilms that are complex structures composed of multiple cells which provide a protective environment for the bacteria to thrive. The compound identified can hence be used in synergy with low doses of first-line drugs to further enhance the activity.

GC-MS analysis of the bioactive fraction showed presence of alkaloids, flavones, anthraquinones and terpenoids.The precursor of the compound 9,10-Anthracenedione1,8-dimethoxy, identified from GC-MS, 9,10 anthacenedione, has been studied earlier as similar structure for mitoxantrone (anthroquinone) that focuses mainly on dividing cells such ascancer cells. The analogous compounds also have cell wall protein inhibiting activity studied *in silico* against *Pseudomonas aeruginosa* proteins[42]. The compound 1,5-Diphenyl-2H-1,2,4-triazoline-3-thione has been identified from leaves of *Gomphandra tetrandra* and has the ability as neuroactivity towards important Alzheimer'sprotein when studied *in silico*[43].

Schisandrin B (lignan compound) identified commonly from *Schisandra chinensis* plant has proven to be hepatoprotective and nephroprotective against TB drugs induced damage *in vitro*. This is due to the strong anti-oxidant property of the compound[44].

7,8,4'-Trihydroxyisoflavone (8-hydroxydaidzin) is an isoflavone, which is a conjugate of daidzein, known for its hepatoprotective, anti-inflammatory and anti-oxidant activity. They function by downregulating crucial factors of inflammationsuch as NFkB in LPS induced Murine cell lines[45]. Iridin is a well-known isoflavone class compound initially derived from *Belamcanda chinensis*. It exerts a strong anti-inflammatory, anti-oxidant, cardio protective activity etc.,Iridin was proven as an effective hepatoprotective agent when treated against LPS induced toxicity in mouse cell lines[46].Spironolactone is a synthetic corticosteroid compound that has prominent biological activity in treating heart related problems, and mainly as an anti-androgen agent. It is also known for its nephroprotective activity proven in clinical samples[47].

3-chloro-N-[2,3-dihydro-1,4-benzodioxan-6-yl)-1, 3-thiazol-2-yl]benzenesulfonamide (Hit3) is an analogue of a synthetic isomer that is generally not found in natural sources of plants, constitute a significant class of drugs known for their antibacterial, anti-carbonic anhydrase, anti-diabetic (hypoglycemic)and antithyroid properties. Synthesis and *in vitro* efficiency of many benzenesulfonamide derivates as targeted therapy have been studied[48]. This analogue of the compound is found to be active in a clinical study, for targeting mammalian amine oxidase enzyme in an attempt to treat neurological disorders[49]. It is also active in a study involving targeting lysine specific demethylase 1 enzyme carried out in THP-1 (Lung) cell lines. However, The potential of this compound is yet to be discovered in tuberculosis treatment[50]. Results, indicates a multi-targeted approach where Hit3 compound interacts with all the selected proteins, shows striking results which can be seen in terms of protein stability and hydrogen bond formation. From the current study, it can be postulated that the fraction VnPeF1 and the compounds predicted by GC-MS analysis exhibited excellent anti-TB activity assessed by various parameters. However, furtheranalysis needs to be done to identify the exact target and mechanism of inhibition in resistant strains of *Mtb*.

Conclusion

In the current study, petroleum ether extract of Vn was analysed using various techniques to identify the anti-TB potential. It is evident from the study that the partially purified compounds isolated from petroleum ether extract of Vn has proven to be potent against *M. smegmatis.* Most of the compounds identified from GC-MS analysis have biological significance related to hepatoprotective activity, in addition to their highlight in anti-oxidant and anti-inflammatory activity. The compounds identified may not be directly related to killing of the bacteria rather they can disrupt the bacterial cell wall integrity leading to cell wall damage and death. In this study, the identified compound mixture has potent anti-tubercular activity at a very low concentration of 12.5 µg/mL identified by REMA assay, maximum inhibition at 8 h observed at 50 µg/mL by time-dependent kill assay and anti-biofilm activity at a concentration of 6.5 µg/mL, respectively. Although Vn has been widely identified with hepatoprotective activities, the in-depth identification of the particular compound(s) responsible for the anti-TB activity are yet to be unravelled. Hence, this study can be considered as a starting point for identifying the compounds that are responsible for its biological significance in treating tuberculosis. The prediction of more than one compound in VnPeF1 by GC-MS, indicates the possibility of synergistic activity of the compounds present in the extract. The strong interaction of Hit3 with the proteins chosen in the study *viz*., MabA, FabD, HadAB and KasA identified using *in silico* analysis, indicates that the compound is potent in targeting more than one aspect of mycolic acid synthesis pathway in *Mtb*. This multi-targeted approach could facilitate the complete elimination of replicating and non-replicating *Mtb* cells, since cell wall synthesis is hindered. However, the individual compound's potential and exact mechanism of inhibition are further to be identified *in vitro* and in resistant strains of *Mtb.*

Acknowledgement

The authors would like to thank Dr. C. Rajasekaran, Professor, School of Bio-Sciences and Technology, Vellore Institute of Technology for authenticating the plant sample. The authors thank Vellore Institute of Technology (VIT) for providing with facilities and infrastructure for carrying out the study. The authors thank the Central Instrumentation Facility, IISc, Bangalore for carrying out GC-MS analysis.

Conflict of interest

The authors declare no conflict of interest.

References

1 *Global tuberculosis report. World Health organisation* Geneva (2023).

2 Chandra P, Grigsby SJ & Philips JA, Immune evasion and provocation by Mycobacterium tuberculosis. *Nat Rev Microbiol*, 20 (2022) 750.

3 Dragset MS, Ioerger TR, Zhang YJ, Mærk M, Ginbot Z, Sacchettini JC, Flo TH, Rubin EJ & Steigedal M, Genome-wide Phenotypic Profiling Identifies and Categorizes Genes Required for Mycobacterial Low Iron Fitness. *Sci Rep*, 9 (2019) 1.

4 Blanc L, Gilleron M, Prandi J, Song O, Jang M, Gicquel B & Drocourt D, Mycobacterium tuberculosis inhibits human innate immune responses via the production of TLR2 antagonist glycolipids. *Immunol Inflamm*, 114 (2017) 11205.

5 Gygli SM, Borrell S, Trauner A & Gagneux S, Antimicrobial resistance in Mycobacterium tuberculosis : mechanistic and evolutionary perspectives. *FEMS Microbiol Rev*, 41 (2017) 354.

6 Jiang CH, Gan ML, An TT & Yang ZC, Bioassay-guided isolation of a Mycobacterium tuberculosis bioflim inhibitor from Arisaema sinii Krause. *Microb Pathog*, 126 (2019) 351.

7 Bhunu B, Mautsa R & Mukanganyama S, Inhibition of biofilm formation in Mycobacterium smegmatis by Parinari curatellifolia leaf extracts. *BMC Complement Altern Med*, 17 (2017) 1.

8 Salomon CE & Schmidt LE, Natural Products as Leads for Tuberculosis Drug Development. *Curr Top Med Chem*, 12 (2012) 735.

9 Xu Y, Liang B, Kong C & Sun Z, Review Article Traditional Medicinal Plants as a Source of Antituberculosis Drugs : A System Review. *Biomed Res Int*, (2021) 1.

10 Sivapalan S, Dharmalingam S, Ashokkumar V, Venkatesan V& Angappan M, Evaluation of the anti-inflammatory and antioxidant properties and isolation and characterization of a new bioactive compound, 3,4,9-trimethyl-7-propyldecanoic acid from *Vitex negundo*. *J Ethnopharmacol*, 319 (2024).

11 Abidin L, Ahmad A, Mir SR, Mujeeb M & Khan SA, Ethnobotany, phytochemistry and pharmacological potential of *Vitex negundo* L. (five-leaved chaste tree): An updated review. *J Coast Life Med*, 3 (2015) 826.

12 Sundarsingh JA, J R, Rajan A & Shankar V, Features of the biochemistry of Mycobacterium smegmatis, as a possible model for Mycobacterium tuberculosis. *J Infect Public Health*, 13 (2020) 1255.

13 Dong Y, Qiu X, Shaw N, Xu Y, Sun Y, Li X, Li J & Rao Z, Molecular basis for the inhibition of β-hydroxyacyl-ACP dehydratase HadAB complex from mycobacterium tuberculosis by flavonoid inhibitors. *Protein Cell*, 6 (2015) 504.

14 Dong Y, Li J, Qiu X, Yan C & Li X, Expression, purification and crystallization of the (3R)-hydroxyacyl-ACP dehydratase HadAB complex from Mycobacterium tuberculosis. *Protein Expr Purif*, 114 (2015) 115.

15 Cantaloube S, Veyron-Churlet R, Haddache N, Daffé M & Zerbib D, The Mycobacterium tuberculosis FAS-II dehydratases and methyltransferases define the specificity of the mycolic acid elongation complexes. *PLoS One*, 6 (2011).

16 Ladda P & Magdum CS, Antitubercular activity and isolation of chemical constituents from plant *Vitex negundo* linn. *Iran J Pharm Res*, 17 (2018) 1353.

17 Singh AK & Reyrat JM, Laboratory maintenance of mycobacterium smegmatis. *Curr Protoc Microbiol*, 14 (2009) 1.

18 Harborne JB, *Phytochemical methods: a guide to modern techniques of plant analysis* Chapman & Hall, UK.

19 François N, Charity NM, Fred O, Meryl C, Nicholas A, Jones OM & Elizabeth MK, Antimycobacterial activities, cytotoxicity and phytochemical screening of extracts for three medicinal plants growing in Kenya. *J Med Plants Res*, 14 (2020) 129.

20 Rajiniraja M & Jayaraman G, Bioautography guided screening of selected indian medicinal plants reveals potent antimycobacterial activity of allium sativum extracts-implication of non sulfur compounds in inhibition. *Int J Pharm Pharm Sci*, 6 (2014) 671.

21 Gopi K, Renu K, Sannanaik Vishwanath B & Jayaraman G, Protective effect of Euphorbia hirta and its components against snake venom induced lethality. *J Ethnopharmacol*, 165 (2015) 180.

22 Ingle KP, Deshmukh AG, Padole DA, Dudhare MS, Moharil MP & Khelurkar VC, Phytochemicals: Extraction methods, identification and detection of bioactive compounds from plant extracts. *J Pharmacogn Phytochem*, 6 (2017) 32.

23 Muniyan R & Jayaraman G, Lauric acid and myristic acid from Allium sativum inhibit the growth of Mycobacterium tuberculosis H37Ra: *in silico* analysis reveals possible binding to protein kinase B. *Pharm Biol*, 54 (2016) 2814.

24 Oladosu, P, Isu, N.R, Ibrahim, K, Okolo, P, Oladepo D., Time Kill-kinetics antibacterial study of Acacia nilotica. In *Theory and Applications of Microbiology and Biotechnology Vol. 2* pp. 56–62. Nigeria.

25 Mothiba MT, Anderson R, Fourie B, Germishuizen WA & Cholo MC, Effects of clofazimine on planktonic and biofilm growth of Mycobacterium tuberculosis and Mycobacterium smegmatis. *J Glob Antimicrob Resist*, 3 (2015) 13.

26 Uzma F, Chowdappa S, Roy A, Adhoni SA, Ali D, Sasaki K & Jogaiah S, GC-MS-Guided Antimicrobial Defense Responsive Secondary Metabolites from the Endophytic Fusarium solani Isolated from Tinospora cordifolia and Their Multifaceted Biological Properties. *Appl Biochem Biotechnol*, 196 (2024) 3010.

27 Boyle NMO, Banck M, James CA, Morley C, Vandermeersch T & Hutchison GR, Open Babel : An open chemical toolbox. (2011) 1.

28 Sundararajan S, Karunakaran K & Muniyan R, Structure based virtual screening and discovery of novel inhibitors against FabD protein of Mycobacterium tuberculosis. *J Biomol Struct Dyn*, 0 (2023) 1.

29 Sander T, Freyss J, Von Korff M & Rufener C, DataWarrior: An open-source program for chemistry aware data visualization and analysis. *J Chem Inf Model*, 55 (2015) 460.

30 Abraham MJ, Murtola T, Schulz R, Páll S, Smith JC, Hess B & Lindah E, Gromacs: High performance molecular simulations through multi-level parallelism from laptops to supercomputers. *SoftwareX*, 1–2 (2015) 19.

31 Schüttelkopf AW & Van Aalten DMF, PRODRG: A tool for high-throughput crystallography of protein-ligand complexes. *Acta Crystallogr Sect D Biol Crystallogr*, 60 (2004) 1355.

32 Nyamweya B, Rukshala D, Fernando N, de Silva R, Premawansa S & Handunnetti S, Cardioprotective Effects of *Vitex negundo*: A Review of Bioactive Extracts and Compounds. *J Evid-Based Integr Med*, 28 (2023) 1.

33 Karakoti H, Mahawer SK, Tewari M, Kumar R, Prakash O, de Oliveira MS & Rawat DS, Phytochemical Profile, *In vitro* Bioactivity Evaluation, *In silico* Molecular Docking and ADMET Study of Essential Oils of Three Vitex Species Grown in Tarai Region of Uttarakhand. *Antioxidants*, 11 (2022).

34 Tandon VR, Khajuria V, Kapoor B, Kour D & Gupta S, Hepatoprotective activity of *Vitex negundo* leaf extract against anti-tubercular drugs induced hepatotoxicity. *Fitoterapia*, 79 (2008) 533.

35 Gupta VK, Shukla C, Bisht GRS, Saikia D, Kumar S & Thakur RL, Detection of anti-tuberculosis activity in some folklore plants by radiometric BACTEC assay. *Lett Appl Microbiol*, 52 (2010) 33.

36 Shettar, Hiremath KV, Anti-proliferative Activity of *Vitex negundo* Leaf Extracts on PA1 Human Ovarian Cancer Cell Lines. *Arch Razi Inst J*, 79 (2024) 426.

37 Muniyan R, Varatharajan S, Naz S, Nandicoori VK & Gurunathan J, Allium Sativum Linn. contains Linear Alkylbenzene sulfonates that alter membrane fluidity for the inhibition of Mycobacterium tuberculosis H37Ra. *Asian J PharmClin Res,*10 (2017).

38 Pawar S & Kamble V, Phytochemical Screening, Elemental and Functional Group Analysis of *Vitex negundo* L. Leaves. *Int J Pharm Pharm Sci*, 9 (2017) 226.

39 Martin A, Camacho M, Portaels F & Palomino JC, Resazurin Microtiter Assay Plate Testing of Mycobacterium tuberculosis Susceptibilities to Second-Line Drugs: Rapid, Simple, and Inexpensive Method. *Antimicrob Agents Chemother*, 47 (2003) 3616.

40 Nyambuya T, Mautsa R & Mukanganyama S, Alkaloid extracts from Combretum zeyheri inhibit the growth of Mycobacterium smegmatis. *BMC Complement Altern Med*, 17 (2017) 1.

41 Palaninathan PS, Raveendran AS & Kesavan JS, Evaluation of the antibacterial efficacy of Vitex negudno leaf extracts against antibiotic resistant Klebseiella pneumoniae an invitro pharmacological study. *Int J Nutr Pharmacol Neurol Dis*, 12 (2022) 319.

42 Adekunle OD, Adeleke OA, Odugbemi AI, Faboro EO & Lajide L, *In vitro* and *in silico* screening and identification of potential bioactive anthraquinones of Morinda lucida benth against pathogenic bacterial target proteins. *Discov Appl Sci*, 6 (2024) 1.

43 Rahman S, Zilani NH, Islam A & Hasan M, In Vivo Neuropharmacological Potential of Gomphandra tetrandra (Wall.) Sleumer and *In silico* study against B-amyloid precursor protein. *Processes*, 9 (2021) 1.

44 Cheng L, Yang Z, Sun Z, Zhang W, Ren Y, Wang M, Han X, Fei L, Zhao Y, Pan H, Xie J & Nie S, Schizandrin B mitigates rifampicin-induced liver injury by inhibiting endoplasmic reticulum stress. *Biol Pharm Bull*, 43 (2020) 145.

45 Hsiao YH, Ho CT & Pan MH, Bioavailability and health benefits of major isoflavone aglycones and their metabolites. *J Funct Foods*, 74 (2020) 0.

46 Ying ZH, Li HM, Yu WY & Yu CH, Iridin prevented against lipopolysaccharide-induced inflammatory responses of macrophages via inactivation of pkm2-mediated glycolytic pathways. *J Inflamm Res*, 14 (2021) 341.

47 Grant P & Ramasamy S, An update on plant derived anti-androgens. *Int J Endocrinol Metab*, 10 (2012) 497.

48 Chundawat NS, Shanbhag GS & Chauhan NPS, Chemical synthesis and molecular modeling of novel substituted N-1,3-benzoxazol-2yl benzene sulfonamides as inhibitors of inhA enzyme and Mycobacterium tuberculosis growth. *J Iran Chem Soc*, 18 (2021) 903.

49 Sommer N & Schulz R, Mitochondrial monoamine oxidase: Another player in pulmonary hypertension? *Am J Respir Cell Mol Biol*, 64 (2021) 277.

50 Hitchin JR, Blagg J, Burke R, Burns S, Cockerill MJ, Fairweather EE, Hutton C, Jordan AM, McAndrew C, Mirza A, Mould D, Thomson GJ, Waddell I & Ogilvie DJ, Development and evaluation of selective, reversible LSD1 inhibitors derived from fragments. *Medchemcomm*, 4 (2013) 1513.